GluR3 Flip and Flop: Differences in Channel Opening Kinetics[†]

Weimin Pei, Zhen Huang, and Li Niu*

Department of Chemistry and Center for Neuroscience Research, University at Albany, SUNY, Albany, New York 12222

Received October 25, 2006; Revised Manuscript Received November 27, 2006

ABSTRACT: Ample evidence from earlier studies of α-amino-3-hydroxy-5-methyl-4-isoxazolepropionic acid (AMPA) receptors, GluR3 included, suggests that alternative splicing not only enriches AMPA receptor diversity but also, more importantly, creates receptor variants that are functionally different. However, it is not known whether alternative splicing affects the receptor channel opening that occurs in the microsecond time domain. Using a laser-pulse photolysis technique combined with whole-cell recording, we characterized the channel opening rate process for two alternatively spliced variants of GluR3, i.e., $GluR3_{flip}$ and $GluR3_{flop}$. We show that the alternative splicing that generates flip and flop variants of GluR3 receptors regulates the channel opening process by controlling the rate of channel closing but not the rate of channel opening or the glutamate binding affinity. Specifically, the flop variant closes its channel almost 4-fold faster than the flip variant. We therefore propose that the function of the flip−flop sequence module in the channel opening process of AMPA receptors is to stabilize the open channel conformation, presumably by its pivotal structural location. Furthermore, a comparison of the flip isoform among all AMPA receptor subunits, based on the magnitude of the channel opening rate constant, suggests that GluR3 is kinetically more similar to GluR2 and GluR4 than to GluR1.

As a post-transcriptional regulatory mechanism (*1*), alternative splicing generates two molecular entities known as "flip" and "flop" in each of the four AMPA[1] receptor subunits, i.e., GluR1−4 or GluRA−D (*2*). The alternative splicing correlates to a 38-amino acid sequence in the extracellular binding domain between the M3 and M4 transmembrane segments but results in a difference of only 9−11 amino acids between the flip and flop isoforms (*2*). Since its discovery in AMPA receptors (*2*), the alternative splicing has been recognized as a unique molecular determinant giving rise to both structural and functional diversities in AMPA receptors (*3*−*6*). For example, flop variants desensitize (i.e., become inactivated when glutamate remains bound to the receptor) at least 3 times faster than the flip counterparts for GluR2−4 (*7*). Flip and flop variants have different sensitivity to allosteric modulators, such as cyclothiazide (CTZ) (*8*−*10*) and metal ions (*11*, *12*). In the brain, the expression of alternatively spliced variants is tissue-, cell type-, and age-dependent (*2*, *7*, *13*, *14*). In some neurological disorders, the relative level of expression of the flip to the flop isoforms is aberrant (*15*−*18*). For instance, in the spinal motor neurons of patients with amyotrophic lateral sclerosis (ALS), the level of the AMPA receptor flip variants is significantly elevated relative to that of the flop variants (*18*). Such an increase in the level of flip isoform expression is thought to make those neurons especially vulnerable to glutamate insult (*18*, *19*).

Despite a wealth of knowledge about alternative splicing, whether it affects the channel opening process of AMPA receptors is currently unknown. To address this question, we focus our initial attention on characterizing the channel opening kinetics for the two alternatively spliced variants of the GluR3 AMPA receptor, i.e., $GluR3_{flip}$ and $GluR3_{flop}$.

GluR3 plays a specific functional role in the central nervous system. For instance, GluR3 assembled with GluR2, one of the two major AMPA receptor populations in adult hippocampus, strengthens the synapses and stabilizes long-term changes in synaptic efficacy (*20*). The level of expression of GluR3 in the hippocampus, together with GluR1 and GluR2 but not with GluR4, increases with development (*21*). GluR3 is also involved in neurological diseases. For instance, the production of autoantibodies against GluR3 contributes to the etiology of several types of human epilepsies (*22*, *23*). Interestingly, GluR3 is expressed on the surface of most normal, cancerous, and autoimmune-associated T cells (*24*). Furthermore, GluR3 is upregulated in the spinal cord of transgenic mice with the copper zinc superoxide dismutase (SOD1) mutation (G93A), a familial ALS mouse model (*25*). At the molecular level, GluR3 is less well understood than other AMPA receptor subunits. For instance, the mean lifetime of the GluR3 open channel, determined traditionally using single-channel recording, is lacking, unlike other AMPA receptor subunits (*26*−*28*). Thus far, there is no systematic study of the phosphorylation of GluR3 (*6*), yet such studies have revealed how phosphorylation can modu-

[†] This work was supported by grants from the Department of Defense (W81XWH-04-1-0106), the ALS Association, and the Muscular Dystrophy Association (to L.N.). Z.H. is supported by a postdoctoral fellowship from the Muscular Dystrophy Association.

* To whom correspondence should be addressed. Telephone: (518) 591-8819. Fax: (518) 442-3462. E-mail: lniu@albany.edu.

[1] Abbreviations: AMPA, α-amino-3-hydroxy-5-methyl-4-isoxazolepropionic acid; ALS, amyotrophic lateral sclerosis; CTZ, cyclothiazide; GFP, green fluorescent protein; HEK-293 cells, human embryonic kidney cells; TAg, large T-antigen.

10.1021/bi062213s CCC: $37.00
Published on Web 01/27/2007

late the receptor properties in trafficking, surface expression, and synaptic plasticity in other AMPA receptor subunits (*6*).

Here we report the kinetic characterization of the channel opening rate constants for $GluR3_{flip}$ and $GluR3_{flop}$ variants using a laser-pulse photolysis technique, together with a photolabile precursor of glutamate [*γ-O*-(α-carboxy-2-nitrobenzyl)glutamate] or caged glutamate. Photolysis of the caged glutamate rapidly liberates free glutamate with a $t_{1/2}$ of ~30 μs (*29*). Using this technique, we previously characterized the channel opening kinetic mechanism for the flip variants of GluR1, GluR2, and GluR4 AMPA receptor channels (*30*−*32*). Thus, this work also completed a systematic study of all flip AMPA receptor variants. We found that the alternative splicing affects the channel opening process by controlling the rate of channel closing but not the rate of channel opening. Specifically, the flop variant shuts the channel almost 4-fold faster than the flip variant. Furthermore, both the flip and flop channels of GluR3, like GluR2 and GluR4, but unlike GluR1, are among some of the fastest channels known to date.

EXPERIMENTAL PROCEDURES

cDNA Expression and Cell Culture. The cDNAs encoding rat $GluR3_{flip}$ and $GluR3_{flop}$ separately in the pBluescript vector were provided by S. Heinemann and were individually cloned into pcDNA3.1 (Invitrogen, Carlsbad, CA). The $GluR3_{flip}$ or $GluR3_{flop}$ homomeric channels were transiently expressed in human embryonic kidney (HEK) 293S cells. HEK-293S cells were cultured in Dulbecco's modified Eagle's medium supplemented with 10% fetal bovine serum in a 37 °C, 5% CO_2, humidified incubator. Unless otherwise noted, HEK-293S cells were also cotransfected with a plasmid encoding green fluorescent protein (GFP) and another plasmid encoding simian virus 40 large T-antigen (TAg) (*33*). GFP was used as a transfection marker for cell recording; TAg was used to potentiate the GluR3 expression (see the text). The weight ratio of the plasmid for GFP and TAg to that of GluR3 was 1:3:30, and the GluR3 cDNA used for transfection was ~15−20 μg/35 mm dish. Cells were used 48 h after transfection.

Whole-Cell Recording. All experiments were preformed with HEK-293S cells voltage-clamped at −60 mV and 22 °C. The recording of glutamate-induced whole-cell current was described previously (*30*). In brief, an Axopatch-200B amplifier (Axon Instruments, Union City, CA) was used in whole-cell recording at a cutoff frequency of 2−20 kHz by a built-in, eight-pole Bessel filter and digitized at a 5−50 kHz sampling frequency with a Digidata 1322A device (Axon Instruments). The resistance of recording electrodes was ~3 MΩ when filled with the electrode solution containing 110 mM CsF, 30 mM CsCl, 4 mM NaCl, 0.5 mM $CaCl_2$, 5 mM EGTA, and 10 mM HEPES (pH 7.4 adjusted with CsOH). The external bath solution contained 150 mM NaCl, 3 mM KCl, 1 mM $CaCl_2$, 1 mM $MgCl_2$, and 10 mM HEPES (pH 7.4 adjusted with NaOH). The GFP fluorescence in transfected cells was visualized using a Zeiss (Thornwood, NY) Axiovert S100 microscope with a fluorescence detection system. To initiate whole-cell current response, solutions containing free glutamate were applied using a flow device (*30*, *34*), and the rise time was typically

$$A + nL \underset{}{\overset{K_1}{\rightleftharpoons}} AL_n \underset{k_{cl}}{\overset{k_{op}}{\rightleftharpoons}} \overline{AL_n}$$

FIGURE 1: General mechanism of channel opening for GluR3. Here, A represents the active, unliganded form of the receptor, L the ligand or glutamate, AL_n the closed channel states with *n* ligand molecules bound, and $\overline{AL_n}$ the open channel states. The number of glutamate molecules to bind to the receptor and to open its channel, *n*, can be from 1 to 4, assuming that a recombinant GluR3 receptor channel is a tetrameric complex, and each subunit has one glutamate binding site. It is further assumed that a ligand does not dissociate from the open channel state. k_{op} and k_{cl} are the channel opening and channel closing rate constants, respectively. For simplicity and without contrary evidence, it is assumed that glutamate binds with equal affinity or K_1, the intrinsic equilibrium dissociation constant, at all binding steps.

~1−2 ms (10−90%). When free glutamate was used, the whole-cell current was corrected for desensitization during the rise time by a previously described method (*34*).

Laser-Pulse Photolysis. The use of the laser-pulse photolysis technique and the caged glutamate (*29*) (Invitrogen, Carlsbad, CA) to measure the rate of an AMPA receptor channel opening with a time resolution of ~60 μs were described previously (*30*). Briefly, a Minilite II pulsed Q-switched Nd:YAG laser (Continuum, Santa Clara, CA) delivered single pulses at 355 nm, tuned by a third harmonic generator, with a pulse length of 8 ns. The laser light was coupled to a fiber optic, and the energy was adjusted to 200−800 μJ. To determine the concentration of glutamate photolytically released from the caged glutamate, at least two solutions with known concentrations of free glutamate were used to calibrate the current amplitude from the same cell before and after a laser pulse. The current amplitudes obtained from the flow measurements were compared with the amplitude from the laser measurement with reference to the dose−response relation. In addition, the concentration of photolytically released glutamate was considered constant during the rise time in which the observed rate constant was measured (see Figure 4A; the k_{obs} was determined from the rise time of <1 ms). In 1 ms, for instance, a glutamate molecule could have only diffused a root-mean-square distance of ~1.2 μm, estimated by Fick's second law, yet the laser irradiation area around a HEK-293 cell of ~10 μm in diameter was 400−500 μm. Thus, the diffusion of glutamate after photolysis, but within the time frame of our measurement of channel opening rate constants, was inconspicuous. It should be noted that in this estimate, we assumed the diffusion coefficient of glutamate was 7.5×10^{-6} cm^2/s, based on the measured value for glutamine at room temperature (*35*).

Data Analysis. On the basis of the kinetic mechanism of channel opening in Figure 1, the observed rate constant, k_{obs}, for the whole-cell current rise in response to glutamate is given by eq 1

$$k_{obs} = k_{cl} + k_{op}\left(\frac{L}{L + K_1}\right)^n \quad (1)$$

All of the terms are defined in the legend of Figure 1. In the derivation of eq 1, the ligand binding rate was assumed to be fast relative to the channel opening rate. This assumption was supported by the consistent observation of

a single first-order rate process for the whole-cell current rise (see the results and discussion in the text), given by eq 2

$$I_t = I_{max}(1 - e^{-k_{obs}t}) \quad (2)$$

where I_t represents the whole-cell current amplitude at time t and I_{max} represents the maximum current amplitude. Using eq 2, the k_{obs} at a given glutamate concentration was calculated. A set of k_{cl} and k_{op} values corresponding to a particular number of ligand(s) required to bind and open the channel, i.e., $n = 1-4$, was obtained using eq 1. Furthermore, K_1 was separately estimated from the dose−response relationship, using eq 3; the derivation of eq 3 was based on the general mechanism of channel opening in Figure 1.

$$I_A = I_M R_M \frac{L^n}{L^n + \Phi(L + K_1)^n} \quad (3)$$

where I_A represents the current amplitude, I_M the current per mole of receptor, R_M the number of moles of receptors on the cell surface, and Φ^{-1} the channel opening equilibrium constant. Other terms have already been defined. The corrected current amplitude (*31*, *34*) was used to construct the dose−response relationship. Unless otherwise noted, triplicate data from three cells were collected in all measurements. Linear regression and nonlinear fitting were performed using Origin version 7 (Origin Lab, Northampton, MA).

RESULTS

Expression of GluR3 in HEK-293 Cells and Whole-Cell Current Recording. We first established a condition under which the GluR3 receptor could be sufficiently expressed in HEK-293 cells for whole-cell recording even at low glutamate concentrations. Earlier studies of GluR3 are primarily involved in the use of *Xenopus* oocytes (*36*, *37*), where the expression of the receptor is more readily detectable but typically at the cost of obscuring the rapid channel desensitization and thus an accurate measurement of the receptor response; this is apparently due to the sheer size of an oocyte. Although using smaller HEK-293 cells achieves a better solution exchange rate, thus permitting a more accurate study of the kinetic properties of GluR3, a lower level of expression in single HEK-293 cells is entailed. Perhaps it is not coincidental that very few studies of GluR3 have used HEK-293 cells for expression, and when those studies were actually performed, often a high glutamate concentration was required to elicit a detectable response. In fact, we observed the average response at saturating concentrations of glutamate was ∼130 pA for $GluR3_{flip}$-expressing HEK-293 cells, similar to literature values (*38*). A small magnitude of whole-cell current response presented a challenge in measuring the GluR3 channel activity at low agonist concentrations, which was required in our experiment to measure the channel closing rate constant (the rationale is presented below).

To improve the receptor expression in single HEK-293 cells and consequently augment the average magnitude of a whole-cell response, we coexpressed TAg with the GluR3 receptor (Figure 2A). TAg is a powerful oncoprotein capable of disrupting cell cycle control (*39*). Coexpression of TAg

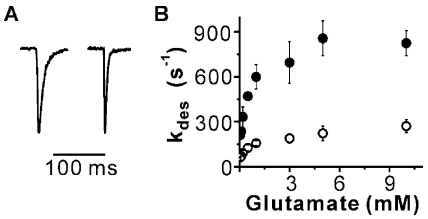

FIGURE 2: Glutamate-induced whole-cell response of $GluR3_{flip}$ and $GluR3_{flop}$ expressed in HEK-293 cells. (A) Representative whole-cell current responses via $GluR3_{flip}$ channels (left) and $GluR3_{flop}$ channels (right) to application of 500 μM glutamate. The amplitude of the current response is 520 and 370 pA for the flip and flop channels, respectively, but the two traces are scaled vertically for comparison of the desensitization rate profile. The $GluR3_{flop}$ channel was desensitized with a rate constant of 470 s^{-1} at this glutamate concentration, whereas the $GluR3_{flip}$ channel was desensitized with a rate constant of only 130 s^{-1}. Note that a first-order rate was adequate for describing the desensitization for both isoforms of GluR3. (B) Dependence of the desensitization rate constant (k_{des}) on glutamate concentration for $GluR3_{flip}$ (○) and $GluR3_{flop}$ (●) channels. Each data point is an average of at least three measurements from at least three cells. An error bar represents the standard error of the mean.

increased the average whole-cell response of $GluR3_{flip}$ to glutamate at saturating concentrations to ∼650 pA (the number of cells tested was 20 or $n = 20$), compared to ∼130 pA without TAg ($n = 3$). For $GluR3_{flop}$, which was usually expressed less robustly, the average current amplitude was ∼250 pA ($n = 5$) when TAg was coexpressed. The largest current amplitudes observed for $GluR3_{flip}$ and $GluR3_{flop}$ were 1.9 and 1.7 nA, respectively. As controls, expressing either TAg alone, GFP alone, or the two together in HEK-293S cells, did not lead to current response (*33*). Coexpressing TAg and GFP with GluR3 did not affect the GluR3 activity either, as evidenced by an identical desensitization rate at a given glutamate concentration from cells transfected with GluR3 only and cells additionally transfected with TAg and GFP. These results are therefore consistent with our earlier report of using TAg to successfully potentiate $GluR2Q_{flip}$ expression in HEK-293S cells (*33*). Furthermore, the method we described, i.e., coexpressing TAg in the same cell, made it possible to assay the GluR3 activity at low concentrations of glutamate.

Inspection of the rate of desensitization with different concentrations of glutamate showed that the flop isoform always desensitized more than 3 times faster than the flip isoform (Figure 2A, B). For instance, the largest rate constant we observed for $GluR3_{flip}$ and $GluR3_{flop}$ were 230 and 820 s^{-1}, respectively. These values agree with those obtained using outside-out patches excised from either HEK-293 cells (*38*) or *Xenopus* oocytes (*7*). That the desensitization rate constants we determined are identical to those published previously is further consistent with the fact that coexpressing TAg in the same cells did not affect the GluR3 channel activity.

Characterization of Caged Glutamate with GluR3 Expressed in HEK-293 Cells. To characterize the channel opening rate constants of the GluR3 receptors, we used a laser-pulse photolysis technique, together with the caged glutamate (Figure 3A), which releases free glutamate upon photolysis with a $t_{1/2}$ of ∼30 μs (*29*). To ensure that the receptor kinetics can be measured, the caged glutamate must be biologically inert on the receptor. In a series of experi-

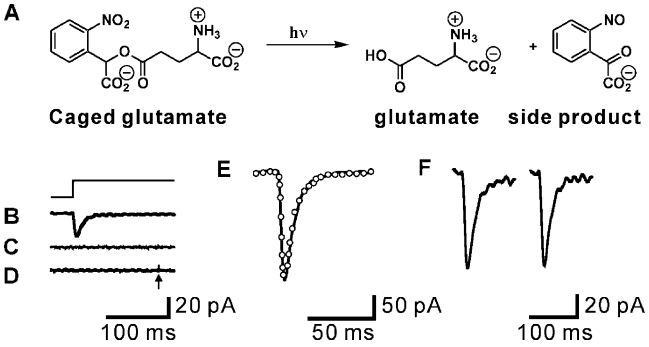

FIGURE 3: Caged glutamate is biologically inert as characterized with $GluR3_{flip}$ expressed in HEK-293 cells voltage-clamped at −60 mV. (A) Photolysis of the caged glutamate releases free glutamate and the side product as shown. (B) Displayed is the whole-cell current response from a cell expressing $GluR3_{flip}$ to 100 μM glutamate. Glutamate (and any other compound or compounds) was applied to the cell using a solution flow device (see Experimental Procedures). The flow-pulse protocol is shown above the current response. (C) The caged glutamate at a concentration of 2 mM (i.e., the highest concentration used in this study), dissolved in the external buffer and applied to the same cell as in panel B, did not induce any detectable whole-cell current response in the absence of laser light. (D) Firing of a laser at a cell exposed to external buffer which contained no caged glutamate did not induce any current response from the cell. The arrow indicates the timing of the laser pulse. (E) Superimposed are the whole-cell current responses to 500 μM free glutamate in the absence (—) and presence (○) of 2 mM caged glutamate from the same cell. The number of the data point for the current trace containing the caged glutamate was reduced for the clarity of presentation. (F) Whole-cell responses to 350 μM free glutamate in the absence (left) and presence (right) of 350 μM side product from photolysis.

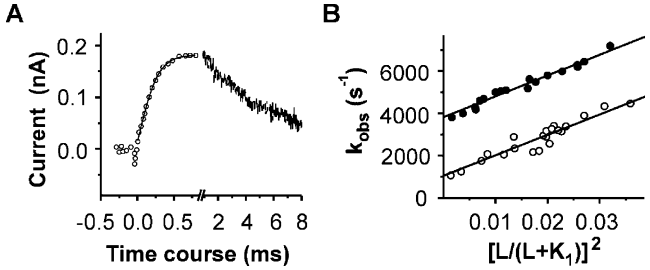

FIGURE 4: Laser-pulse photolysis measurement of the channel opening kinetics for $GluR3_{flip}$ and $GluR3_{flop}$. (A) Representative whole-cell current from the opening of the $GluR3_{flip}$ channel initiated by the laser-pulse photolysis of caged glutamate at time zero. The fitting of the current rise using eq 2 (in Experimental Procedures) is shown as the solid line superimposed with the experimental data points. For clarity, the number of data points was reduced in the rising phase of the current. The observed rate constant (k_{obs}) of 2400 s^{-1} obtained from this trace corresponds to a glutamate concentration of 170 μM. Note that the direction of the current response was plotted as the opposite of that recorded. (B) Plot of k_{obs} vs glutamate concentration by eq 1 in the linear form. The empty circles represent k_{obs} values for $GluR3_{flip}$ and filled circles represent those for $GluR3_{flop}$. Each data point represents one k_{obs} obtained at a particular concentration of photolytically released glutamate. The k_{cl} and k_{op} values were determined by linear fit to be $(1.1 \pm 0.2) \times 10^3$ and $(9.6 \pm 1.1) \times 10^4$ s^{-1} for $GluR3_{flip}$ and $(3.8 \pm 0.1) \times 10^3$ and $(9.9 \pm 0.5) \times 10^4$ s^{-1} for $GluR3_{flop}$, respectively. In the linear fitting, we chose an n of 2; $K_1 = 1.0$ mM for $GluR3_{flip}$ and 0.95 mM for $GluR3_{flop}$.

ments (Figure 3B−F) designed to test the biological properties of the caged glutamate, we found, on the same cell that expressed the GluR3 channel (as seen by a current response to free glutamate, Figure 3B), the caged glutamate did not activate the GluR3 channel without the laser flash (Figure 3C). Firing the laser in the absence of the caged glutamate did not induce current response from cells that expressed GluR3 (Figure 3D). The caged glutamate did not inhibit or potentiate the GluR3 response when the receptor was activated by free glutamate, as evidenced by identical current amplitudes in the presence and absence of caged glutamate (Figure 3E). Furthermore, the side product(s) generated from photolyzing the caged glutamate (Figure 3A) did not affect the glutamate-induced receptor response (Figure 3F). Together, these results show that the caged glutamate was biologically inert and thus suitable for studying the GluR3 channels. This conclusion is consistent with the initial finding with rat hippocampal neurons that expressed endogenous AMPA receptors (*29*) and our previous studies of other AMPA receptors (*30*−*32*).

Rate of Channel Opening. Using the laser-pulse photolysis technique with the caged glutamate, we determined the rate constants for the opening of the $GluR3_{flip}$ and $GluR3_{flop}$ channels. Upon laser photolysis, free glutamate was liberated, leading to a rapid increase in the whole-cell current representing the opening of the receptor channel (Figure 4A). The rising phase of the current obeyed a single-exponential rate throughout the entire concentration range of glutamate (i.e., 80−260 μM), which supported the assumption that the rate of channel opening was slow compared to the rate of glutamate binding. Thus, the observed rate reflected channel opening. The result was inconsistent with the assumption that the channel opening rate was either comparable to or faster than the ligand binding rate (note that all of these kinetic scenarios have been discussed in detail in our previous studies; see ref *31*). Accordingly, a general kinetic rate expression, i.e., eq 1 (in Experimental Procedures), was derived for the observed rate constant, k_{obs}, with n ligand molecules bound to open the channel, AL_n, as a function of ligand concentration.

Using eq 1, we estimated the channel opening rate constant, k_{op}, and the channel closing rate constant, k_{cl}, together with the corresponding K_1 value, from the plot of k_{obs} versus the concentration of glutamate for $GluR3_{flip}$ and $GluR3_{flop}$ (Figure 4B). Table 1 lists four sets of k_{op}, k_{cl}, and K_1 values, corresponding to an n of 1−4. The n of 1−4 was based on the assumption that a recombinant GluR3 receptor is a tetramer (*40*, *41*), and each subunit contains one glutamate binding site. From our results, the following conclusions can be drawn. First, the fitting was satisfactory when n equaled 2−4, but not when n equaled 1 (see R^2 values in Table 1). Second, the fitting results are statistically identical when $n = 2-4$. For instance, when n increased from 2 to 4, the fitted k_{op} changed little (see Table 1). Third, the conclusions described above applied to the kinetic results of both $GluR3_{flip}$ and $GluR3_{flop}$. As an independent estimate of K_1 with respect to different numbers of ligands bound to a receptor complex, we determined the dose−response relationship for both $GluR3_{flip}$ and $GluR3_{flop}$ (Figure 5). Using eq 3, we found that the dose−response relationship of both variants showed a similar pattern in that the fitting was satisfactory when n equaled 2−4 but poor when n equaled 1 (Table 2). Furthermore, a K_1 value obtained from the dose−response curve (Figure 5) agreed with that obtained from kinetic measurement (Figure 4B) at a given n, with

Table 1: k_{op} and k_{cl} Values for $GluR3_{flip}$ and $GluR3_{flop}$ When $n = 1-4$[a]

	$GluR3_{flip}$				$GluR3_{flop}$			
n	k_{op} ($\times 10^{-5}$ s^{-1})	k_{cl} ($\times 10^{-3}$ s^{-1})	K_1 (mM)	R^2	k_{op} ($\times 10^{-5}$ s^{-1})	k_{cl} ($\times 10^{-3}$ s^{-1})	K_1 (mM)	R^2
1	0.20 ± 1.6	1.2 ± 2.0	1.6 ± 16	0.679	0.15 ± 0.10	1.1 ± 1.0	0.34 ± 0.49	0.890
2	0.97 ± 1.2	1.0 ± 0.5	1.0 ± 0.90	0.908	0.99 ± 1.1	3.8 ± 0.3	0.97 ± 0.76	0.970
3	1.1 ± 2.0	1.4 ± 0.9	0.50 ± 0.50	0.901	1.1 ± 1.6	4.1 ± 0.6	0.50 ± 0.50	0.960
4	1.2 ± 1.9	1.7 ± 0.9	0.35 ± 0.25	0.895	1.3 ± 1.9	4.3 ± 0.9	0.33 ± 0.20	0.952

[a] n is the number of glutamate molecules required to bind and open the channel.

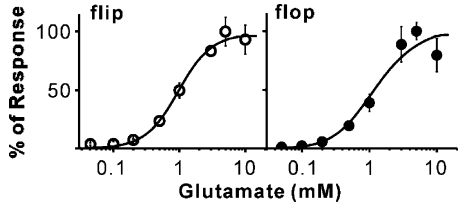

FIGURE 5: Dose−response relationship of the $GluR3_{flip}$ (○) and $GluR3_{flop}$ (●) channels with glutamate. The whole-cell currents from different cells were normalized to the current obtained at 0.5 mM glutamate, and the current amplitude at 5 mM was set to 100%. The solid lines represent the fits when $n = 2$ by eq 3, and the K_1, Φ, and $I_M R_M$ values are listed in Table 2.

the exception, in both isoforms, of an n of 1 (see Tables 1 and 2).

Difference in the Channel Opening Properties of $GluR3_{flip}$ and $GluR3_{flop}$. Comparison of the corresponding set of rate constants, excluding $n = 1$, shows that $GluR3_{flop}$ closes its channel more than 3-fold faster than $GluR3_{flip}$, yet both open their respective channels with an identical rate constant. Therefore, the flip−flop module of GluR3 regulates the channel opening process by controlling how fast the open channel closes. It should be especially emphasized that the same conclusion could be made empirically from k_{obs} without even knowing the values of k_{op} and k_{cl}. If $L \ll K_1$ or at low agonist concentrations, $k_{obs} \approx k_{cl}$ (see eq 1), suggesting that the evaluation of k_{cl} was independent of whatever the n value was (in fact, estimating k_{cl} was independent of the k_{op} term altogether; see eq 1). Thus, that the k_{obs} value of $GluR3_{flip}$ at the low glutamate concentration was 3-fold smaller than that of $GluR3_{flop}$ (in Figure 4B) led naturally to the same conclusion.

Furthermore, both the rate and the dose−response data suggest that K_1 is the same for both GluR3 variants (Tables 1 and 2). For instance, when $n = 2$, K_1 is 1.0 ± 0.70 mM for $GluR3_{flip}$ and 0.95 ± 0.65 mM for $GluR3_{flop}$, suggesting that the flip−flop module does not affect the binding affinity of glutamate. The same conclusion can be qualitatively made from the analysis of the dose−response relationships using the Hill equation (*42*). The EC_{50} value or the ligand concentration that corresponds to 50% of the maximum response is 1.0 ± 0.20 mM for $GluR3_{flip}$ and 1.1 ± 0.30 mM for $GluR3_{flop}$ with Hill coefficients of 1.8 and 1.7, respectively. Again, the EC_{50} values for $GluR3_{flip}$ and $GluR3_{flop}$ are identical. In fact, EC_{50} is similar to K_1 numerically (note that the Hill equation does not specify the number of bound ligand molecules). Interestingly, the flip and flop isoforms of GluR2, another AMPA receptor subunit, also have identical EC_{50} values: 1.39 mM for $GluR2Q_{flip}$ and 1.38 mM for $GluR2Q_{flop}$ (*43*).

The Channel Opening Rate Was Measured Separately from Channel Desensitization. Our analysis of the channel opening kinetics was based on the mechanism for channel opening (Figure 1), which did not involve channel desensitization. We reasoned that the desensitization reaction could not have proceeded appreciably during the current rise, assuming that the desensitization had occurred simultaneously upon binding of glutamate (*44*, *45*). As shown in Figure 4A, the k_{obs} of 2400 s^{-1}, calculated from the current rise for the $GluR3_{flip}$ channel opening, was ~30 times larger than the desensitization rate of 80 s^{-1} in Figure 2B at the same glutamate concentration, i.e., 170 μM. As such, when the current increased to 95%, during which the k_{obs} of 2400 s^{-1} was calculated, the desensitization reaction with a rate constant of 80 s^{-1} proceeded only ~4%. Thus, the kinetic process occurring within the current rising phase was dominated by the channel opening reaction, and its rate constant could be calculated using a simple kinetic rate expression (eq 2). It should be noted that the estimate of the "contamination" of the desensitization reaction within the rise time was reasonably accurate because the receptor was exposed to glutamate in a microsecond "concentration jump" triggered by laser photolysis, and consequently, the start of the glutamate-induced reactions was virtually synchronized. In addition, a simultaneous fit of both the rising and falling phases (in Figure 4A) by two first-order rate equations, one representing channel opening and the other representing desensitization, yielded a k_{obs} value identical (±5% error range) to that obtained using a single-exponential fit of the rising phase only (using eq 2). Together, the whole-cell current rise representing the channel opening reaction can be treated as a kinetically distinct process in our measurement. Indeed, it has been proposed previously that the channel opening reaction or the gating pathway can be considered a kinetic process separate from desensitization (*44*, *46*), and the open channel state is thought to preferentially return to the closed state and can open again, without entering the desensitization state (*47*).

DISCUSSION

We have investigated the kinetic mechanism of channel opening for the two alternatively spliced variants of GluR3. We find the alternative splicing that generates flip and flop variants of GluR3 AMPA receptors controls the channel opening process by regulating the rate of channel closing but not the rate of channel opening. Below, we discuss the use of the channel opening and channel closing rate constants in an effort to understand the receptor properties and offer implications of alternative splicing in regulating the channel function.

Channel Opening Rate Constants and Receptor Occupancy. The results from our study of GluR3 are consistent with the minimal number of glutamate molecules required to bind to and to open the channel being 2 (*30*−*32*). This is

Table 2: K_1 Values Estimated from Dose−Response Curve for $GluR3_{flip}$ and $GluR3_{flop}$

	$GluR3_{flip}$				$GluR3_{flop}$			
n	K_1 (mM)	Φ	I_mR_m (nA)	R^2	K_1 (mM)	Φ	I_mR_m (nA)	R^2
1	2.6 ± 751	0.14 ± 45	88 ± 3479	0.780	7.0 ± 1252	0.12 ± 24	108 ± 2359	0.738
2	1.0 ± 0.70	0.55 ± 0.89	166 ± 90	0.997	0.95 ± 0.65	0.79 ± 0.40	190 ± 130	0.956
3	0.70 ± 0.50	0.35 ± 0.64	141 ± 80	0.990	0.62 ± 1.0	0.68 ± 3.2	177 ± 355	0.955
4	0.36 ± 0.30	0.75 ± 1.5	184 ± 169	0.989	0.43 ± 0.59	0.81 ± 3.6	188 ± 400	0.955

true for both the flip and flop variants (see Table 1). For either of the isoforms, our results show that k_{op} remains essentially invariant when $n = 2-4$ (Table 1). If receptor complexes bound with more than two glutamate molecules have higher conductance levels, then the higher conductance levels associated with higher agonist occupancy do not give rise to different channel opening rate constants. Alternatively, the receptor complexes with higher occupancy have different rate constants of channel opening, but the fraction of these complexes in the overall receptor population all bound with glutamate is not high enough to significantly alter k_{obs} values. It is also possible that the concentration range of glutamate released by photolysis may not be wide enough for our data analysis (in Figure 4B). However, regardless of how k_{obs} is used to calculate k_{op} and k_{cl} with respect to a specific *n* value, the set of k_{op} and k_{cl} values when $n = 2$ is phenomenologically representative of the channel opening kinetics for both $GluR3_{flip}$ and $GluR3_{flop}$. We thus favor an interpretation of k_{op} and k_{cl} with an *n* of 2 being the minimal values of the channel opening and channel closing rate constants.

From the elegant study of the single-channel records of both the wild-type and mutant GluR3 receptors, Rosenmund and co-workers (*40*) suggested that binding of two agonist molecules per tetrameric receptor complex is necessary to open the channel, and binding of more than two agonist molecules leads to the open channels with higher mean single-channel conductance. Evidence that supports this conclusion includes the single-channel study of native AMPA receptors at varying glutamate concentrations (*48*) and the single-channel/crystallographic studies of GluR2 with different agonists (*28*). Given that an AMPA receptor may be a dimer of "dimers" (*49*), binding of one glutamate molecule per dimer or two per tetramer as a minimal stoichiometry is plausible (*32*). Furthermore, despite the fact that channel conductance of AMPA receptors depends on agonist occupancy, it is unclear how a change in conductance affects synaptic response seen as macroscopic current. It has been suggested that glutamate at the synapse may not be able to visit multiple conductance levels of synaptic AMPA receptors (*48*), because glutamate cannot be present in the synaptic cleft at concentrations of >1 mM for more than 100−200 μs or because the channels desensitize rapidly (*50*, *51*).

Alternative Splicing Regulates the GluR3 Channel Opening Process. The channel opening rate constant defines how fast a channel opens following the binding of glutamate. The channel closing rate constant represents how fast an open channel closes and thus is a measure of the lifetime of an open channel with the relationship $k_{cl} = 1/\tau$, where τ is the lifetime expressed as a time constant (*31*). In this study, we determined k_{op} to be 97 000 s^{-1} for $GluR3_{flip}$ and 99 000 s^{-1} for $GluR3_{flop}$ and k_{cl} to be 1000 s^{-1} for $GluR3_{flip}$ and 3800 s^{-1} for $GluR3_{flop}$. On the basis of these results, we conclude that alternative splicing does not affect the channel opening rate reaction but does affect the channel closing rate process of GluR3 in that the flop variant has a markedly faster channel closing rate than the flip counterpart. Furthermore, on the basis that the flip and flop variants have identical K_1 values or EC_{50} values, the alternative splicing may not affect the rate of binding of glutamate to the receptor.

Our findings also reveal how the alternative splicing regulates the channel function. First, at high concentrations of glutamate, the time course is unaffected by alternative splicing, because for GluR3, $k_{op} \gg k_{cl}$, and the time constant of the current rise, i.e., $1/(k_{op} + k_{cl})$, is mainly determined by k_{op}. Second, because alternative splicing mainly affects k_{cl}, it will influence more effectively the channel activity of GluR3 at lower glutamate concentrations. Third, alternative splicing has little influence on the channel opening probability, P_{op}, or the probability that a channel can open once it is bound with ligand(s) (*31*, *52*, *53*). This is because $P_{op} = k_{op}/(k_{op} + k_{cl})$, and again, $k_{op} \gg k_{cl}$. Specifically, the P_{op} values for $GluR3_{flip}$ and $GluR3_{flop}$ are estimated to be 0.99 ± 0.12 and 0.96 ± 0.10, respectively, consistent with a high P_{op} value in general for AMPA receptors (*32*). In fact, because $k_{op} \gg k_{cl}$, P_{op} naturally approaches unity; see $P_{op} = k_{op}/(k_{op} + k_{cl})$, regardless of the *n* value or agonist occupancy. Physiologically, the synaptic concentration of glutamate can be as high as 1 mM (*50*, *54*). Therefore, it is unlikely that alternative splicing plays a significant role in shaping the initial events of synaptic activity when the glutamate concentration is that high.

Given the prediction that the flip−flop module affects channel activity, it is plausible that alternative splicing has a major impact on excitatory postsynaptic current (EPSC) at low glutamate concentrations, such as in the slow-rising component of the AMPA receptor-mediated conductance at the cerebellar mossy fiber-granule cell synapse (*55*). Such a slow synaptic current is mediated possibly by two mechanisms, a prolonged local release of glutamate via a narrow fusion pore and a spillover or the diffusion of glutamate from distant sites (*55*). Both mechanisms may involve a low synaptic glutamate concentration. For example, in the cerebellar mossy fiber-granule cell synapse, a glutamate concentration of ∼130 μM through a spillover mechanism is thought to be responsible for the slow-rising EPSC (*55*). Moreover, both spillover and narrow fusion pore release are believed to play important roles in developmental strengthening of central glutamatergic synaptic connections (*55*, *56*). Under such a condition where low glutamate concentrations are prevalent, the kinetically distinct flip and flop variants may be relevant for synaptic transmission. Furthermore, because the flip isoform dwells on the open channel state longer, more calcium can enter the cell that harbors the flip isoform per unit time. This prediction is consistent with the pathogenic hypothesis by which an elevated level of expres-

sion of the flip isoforms of AMPA receptors in the spinal motor neurons of ALS patients shall render those cells more vulnerable to excitotoxicity (*18*).

The Flip−Flop Alternative Splicing Sequence Is a Structure-Stabilizing Module. Armstrong and Gouaux (*41*, *57*) first proposed that opening of an AMPA channel is initiated by the closure of receptor domains or lobes 1 and 2, after agonist binding, from their X-ray crystallographic study of the S1S2 extracellular binding domains of AMPA receptors. The trapping of agonist bound to the extracellular domains causes a conformational strain in the extracellular portion of the receptor, leading to the opening of the gate in the transmembrane segment (*41*, *58*). Using these structural concepts, the k_{op} obtained for the GluR3 channel may represent the rate of domain closure induced by glutamate binding, and the k_{cl} should then correspond to the rate of re-opening of the bilobe structure to return to its original active conformation. It should be noted that the magnitude of the channel closing rate constant, k_{cl}, or the mean lifetime of the open channel, τ ($k_{cl} = 1/\tau$), reflects the stability of the open channel state of the receptor. Therefore, the flip sequence in the flip−flop alternative splicing module promotes a more stable open channel conformation than does the flop sequence, simply because the k_{cl} of $GluR3_{flip}$ is smaller than that of $GluR3_{flop}$. Consequently, the flip−flop module is hypothesized to operate to "tune" the channel opening equilibrium. It should be pointed out that generally for proteins, substrate-induced conformational changes correlate to rate constants in the range of $10-10^4$ s^{-1} (*59*). Therefore, on the basis of the values of k_{op} and k_{cl} for the GluR3 receptors, the link of k_{op} to the rate of bilobe closure and the link of k_{cl} to the rate of re-opening of the closed bilobe as major conformational changes are plausible.

It is worth noting that the alternatively spliced region of AMPA receptors is located in the S2 extracellular domain or right above the fourth transmembrane domain. Unless its location is accidental, we hypothesize that the alternatively spliced region in AMPA receptors is situated in a pivotal position in that it serves as a structural "lamppost" involved in stabilizing the extracellular binding domain when this domain transiently changes its conformation upon binding to glutamate or when the gate in the transmembrane domain is open. Specifically, if the flip sequence is used as the benchmark, the flop sequence corresponds to a structurally weakened lamppost such that the closed bilobe structure is less stable or the re-opening of this structure is kinetically more favorable as it has a larger k_{cl}. Obviously, further studies are needed to test this hypothesis. If true, the alternative splicing has a structural meaning: it regulates the stability of the open channel conformation.

Time Course for $GluR3_{flip}$ and $GluR3_{flop}$. The time course of channel opening describes the speed by which channels open, defined by k_{op}, and the duration of the open channels, defined by k_{cl}, at a given concentration of ligand for the ensemble rate process (*31*). Consequently, the time course for the opening of $GluR3_{flip}$ and $GluR3_{flop}$ channels can be constructed using k_{cl} and k_{op} values as a function of glutamate concentration, according to eq 1 (in Figure 6). Specifically, the time course was calculated to be the rise time of the whole-cell current increase from 20 to 80%. As expected, when the glutamate concentration increases, the time course decreases and the difference in the time course between the flip and flop variants narrows (Figure 6). This is because at high ligand concentrations, the magnitude of k_{op} dominates the kinetic behavior of the channel, and the k_{op} values for $GluR3_{flip}$ and $GluR3_{flop}$ are identical (regardless of the number of ligand molecules bound to a receptor to open its channel). Consequently, the shortest rise time, which is achieved at a saturating glutamate concentration, is ~14 and ~13 μs for the flip and flop isoforms, respectively.

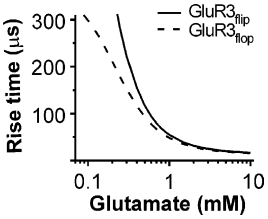

FIGURE 6: Time course for $GluR3_{flip}$ and $GluR3_{flop}$ as a function of glutamate concentration. The time course is expressed as the rise time of the whole-cell current. The rise time is defined as the time for the receptor current response to rise from 20 to 80% and is obtained by converting a k_{obs} value by eq 1, using experimentally determined k_{op} and k_{cl} values at $n = 2$ for a corresponding glutamate concentration.

In the description of the time course, the desensitization was assumed not to occur appreciably in the same period of time, and such an assumption was reasonable as discussed earlier. However, the inclusion of the desensitization rate is needed to define the total time duration (*50*, *60*), which further includes the current falling to the baseline, similar to defining the size and duration of EPSP. Furthermore, to define rigorously an *in vivo* time course, additional factors must be considered, such as the time of glutamate uptake from the synaptic cleft and the relative location of receptors in the postsynaptic density. Other factors that complicate the measurement of an *in vivo* time course include a prolonged local release of glutamate and a slow rise time due to a low synaptic concentration of glutamate. A prolonged local release could occur because the neurotransmitter is released through a narrow fusion pore or because the neurotransmitter is diffused from distant sites, i.e., "spillover" (*55*). A slow rise time has been recorded from AMPA synapses (*56*, *61*−*63*). Therefore, the time course we constructed (Figure 6) only sets the upper limit for the early part of the channel activity, assuming synchronized activation of the receptors at the same location.

When the glutamate concentration is sufficiently low, the rate of glutamate binding becomes rate-limiting because ligand binding is a bimolecular process (Figure 1). Consequently, an observed rate of current rise will no longer reflect the channel opening (*32*). To ensure that the ligand binding rate was fast enough during our laser-pulse photolysis measurement so that the relatively slow channel opening process was always observed, we only used those k_{obs} values that corresponded to glutamate concentrations of ≥ 80 μM for data analysis (in Figure 4B). The glutamate concentration of 80 μM is equivalent to evoking ~4% of the channels (i.e., the fraction of the open channel state in all channel populations, which is defined by eq 3 and shown in Figure 5 for both GluR3 isoforms). This kinetic rationale and the resulting practice have been thoroughly discussed in our previous studies of other AMPA receptor channels (*31*).

Knowing the time course of synaptic conductance is necessary for investigation of information processing in the

Table 3: k_{op} and k_{cl} Values for Some Homomeric Ionotropic Glutamate Channels[a]

glutamate receptor	k_{op} (s^{-1})	k_{cl} (s^{-1})	technique	ref
NR1A/NR2A[b]	77	28	single-channel recording	*68*
$GluR1Q_{flip}$[c,d]	2.9×10^4	2.1×10^3	laser-pulse photolysis	*31*
		4.2×10^3 (73%)	single-channel recording	*27*
		4.2×10^2 (27%)		
$GluR2Q_{flip}$	8.0×10^4	2.6×10^3	laser-pulse photolysis	*30*
		3.1×10^3 (84%)	single-channel recording	*28*
		6.8×10^2 (16%)		
	1.6×10^4	5.0×10^3	fitting	*43*
$GluR3_{flop}$	9.9×10^4	3.8×10^3	laser-pulse photolysis	this study
$GluR3_{flip}$	9.6×10^4	1.1×10^3	laser-pulse photolysis	this study
$GluR4_{flip}$	6.8×10^4	3.4×10^3	laser-pulse photolysis	*32*
	4.0×10^4	8.0×10^3	fitting	*69*
		5.9×10^3	single-channel recording	*26*
GluR6Q	1.1×10^4	4.2×10^2	laser-pulse photolysis	*67*
	1.0×10^4	4.4×10^2	fitting	*52*
	1.0×10^4		flow measurement	*46*

[a] In all data cited, glutamate is the agonist. [b] *Xenopus* oocytes were used for the study of NMDA channels; the rest of the studies were with HEK-293 cells. [c] The k_{op} and k_{cl} values cited in the laser-pulse photolysis measurements are those at $n = 2$. [d] A channel closing rate constant (k_{cl}) obtained from single-channel recording is converted from the mean lifetime of the open channel (τ) via the relationship $k_{cl} = 1/\tau$.

brain, as it determines such basic properties as temporal precision and reliability (*64*, *65*) and the gain of rate-encoded signals (*66*). It is also required to characterize the integration of nerve impulses that arrive at a chemical synapse or that originate from the same synapse but from different receptors or even from different isoforms of the same receptor responding to the same chemical signals, like glutamate. Such a study is especially meaningful for ionotropic glutamate receptors, because all three channel subtypes, namely, NMDA, AMPA, and kainate channels, are known to have different channel opening rate constants in response to the same agonist, glutamate.

Comparison of the Channel Opening Rate Constants of GluR3 with Those of Other Glutamate Receptors. Our study of GluR3 channel opening kinetics also constitutes a complete characterization of the channel opening rate constants for the flip variants of all AMPA receptor channels (Table 3). The comparison of the channel opening kinetics among these receptor subunits reveals clear differences in the channel opening and channel closing rate constants. Most strikingly, the magnitude of the k_{op} values for both $GluR3_{flip}$ and $GluR3_{flop}$ channels suggests that both variants are fast-activating channels, similar to GluR2 and GluR4 but different from GluR1 (see Table 3). Any of the k_{op} values in GluR2−4 are at least 3-fold larger than the k_{op} of GluR1. In terms of K_1 and EC_{50} values, GluR3 is also more similar to GluR2 and GluR4, i.e., ~1 mM (*30*, *32*, *43*), than to GluR1, i.e., ~0.5 mM (*31*). Interestingly, only the flip and flop variants of GluR1 do not exhibit different rates of desensitization (*7*). Our preliminary study of the channel opening kinetics of $GluR1Q_{flop}$ (unpublished data) shows that its k_{cl} and k_{op} values are identical to those of the $GluR1Q_{flip}$ channels (*31*). Together, these results suggest that GluR2, GluR3, and GluR4 are kinetically similar to each other, but different from GluR1.

Because of a relatively low K_1 or EC_{50} for GluR1 compared to other AMPA channels, a greater proportion of the GluR1 channel can open at a given concentration of glutamate, such as 1 mM, albeit with a relatively slower rate, compared with other AMPA channels. This difference is particularly significant when the glutamate concentration is low but disappears when the glutamate concentration reaches saturation with respect to all AMPA channels. However, when k_{cl} is used as a unifying standard for comparison, it is apparent that $GluR3_{flip}$ has the smallest k_{cl}, whereas $GluR4_{flip}$ has the largest k_{cl}; $GluR1Q_{flip}$ and $GluR2Q_{flip}$, on the other hand, seem to have similar k_{cl} values. What this difference means physiologically is not yet known. It is clear, however, that functional differences among these channels should manifest more pronouncedly at lower glutamate concentrations. Finally, with limited information available, all AMPA channels have nevertheless larger channel opening rate constants, compared with the GluR6 kainate receptor channel (*67*) (Table 3). Whether this difference represents general kinetic properties between kainate and AMPA receptors also merits future studies.

ACKNOWLEDGMENT

We are grateful to Steve Heinemann for the GluR3 clones and to anonymous reviewers for insightful comments. We thank Lisa Maroski for editing.

REFERENCES

1. Gallo, J. M., Jin, P., Thornton, C. A., Lin, H., Robertson, J., D'Souza, I., and Schlaepfer, W. W. (2005) The role of RNA and RNA processing in neurodegeneration, *J. Neurosci. 25*, 10372−10375.
2. Sommer, B., Keinanen, K., Verdoorn, T. A., Wisden, W., Burnashev, N., Herb, A., Kohler, M., Takagi, T., Sakmann, B., and Seeburg, P. H. (1990) Flip and flop: A cell-specific functional switch in glutamate-operated channels of the CNS, *Science 249*, 1580−1585.
3. Hollmann, M., and Heinemann, S. (1994) Cloned glutamate receptors, *Annu. Rev. Neurosci. 17*, 31−108.
4. Dingledine, R., Borges, K., Bowie, D., and Traynelis, S. F. (1999) The glutamate receptor ion channels, *Pharmacol. Rev. 51*, 7−61.
5. Erreger, K., Chen, P. E., Wyllie, D. J., and Traynelis, S. F. (2004) Glutamate receptor gating, *Crit. Rev. Neurobiol. 16*, 187−224.
6. Palmer, C. L., Cotton, L., and Henley, J. M. (2005) The molecular pharmacology and cell biology of α-amino-3-hydroxy-5-methyl-4-isoxazolepropionic acid receptors, *Pharmacol. Rev. 57*, 253−277.
7. Mosbacher, J., Schoepfer, R., Monyer, H., Burnashev, N., Seeburg, P. H., and Ruppersberg, J. P. (1994) A molecular determinant for submillisecond desensitization in glutamate receptors, *Science 266*, 1059−1062.

8. Partin, K. M., Patneau, D. K., and Mayer, M. L. (1994) Cyclothiazide differentially modulates desensitization of α-amino-3-hydroxy-5-methyl-4-isoxazolepropionic acid receptor splice variants, *Mol. Pharmacol. 46*, 129−138.
9. Partin, K. M., Fleck, M. W., and Mayer, M. L. (1996) AMPA receptor flip/flop mutants affecting deactivation, desensitization, and modulation by cyclothiazide, aniracetam, and thiocyanate, *J. Neurosci. 16*, 6634−6647.
10. Kessler, M., Rogers, G., and Arai, A. (2000) The norbornenyl moiety of cyclothiazide determines the preference for flip-flop variants of AMPA receptor subunits, *Neurosci. Lett. 287*, 161−165.
11. Shen, Y., and Yang, X. L. (1999) Zinc modulation of AMPA receptors may be relevant to splice variants in carp retina, *Neurosci. Lett. 259*, 177−180.
12. Karkanias, N. B., and Papke, R. L. (1999) Lithium modulates desensitization of the glutamate receptor subtype gluR3 in *Xenopus* oocytes, *Neurosci. Lett. 277*, 153−156.
13. Fleck, M. W., Bahring, R., Patneau, D. K., and Mayer, M. L. (1996) AMPA receptor heterogeneity in rat hippocampal neurons revealed by differential sensitivity to cyclothiazide, *J. Neurophysiol. 75*, 2322−2333.
14. Lambolez, B., Ropert, N., Perrais, D., Rossier, J., and Hestrin, S. (1996) Correlation between kinetics and RNA splicing of α-amino-3-hydroxy-5-methylisoxazole-4-propionic acid receptors in neocortical neurons, *Proc. Natl. Acad. Sci. U.S.A. 93*, 1797−1802.
15. Eastwood, S. L., Burnet, P. W., and Harrison, P. J. (1997) GluR2 glutamate receptor subunit flip and flop isoforms are decreased in the hippocampal formation in schizophrenia: A reverse transcriptase-polymerase chain reaction (RT-PCR) study, *Brain Res. Mol. Brain Res. 44*, 92−98.
16. Stine, C. D., Lu, W., and Wolf, M. E. (2001) Expression of AMPA receptor flip and flop mRNAs in the nucleus accumbens and prefrontal cortex after neonatal ventral hippocampal lesions, *Neuropsychopharmacology 24*, 253−266.
17. Seifert, G., Schroder, W., Hinterkeuser, S., Schumacher, T., Schramm, J., and Steinhauser, C. (2002) Changes in flip/flop splicing of astroglial AMPA receptors in human temporal lobe epilepsy, *Epilepsia 43*, 162−167.
18. Tomiyama, M., Rodriguez-Puertas, R., Cortes, R., Pazos, A., Palacios, J. M., and Mengod, G. (2002) Flip and flop splice variants of AMPA receptor subunits in the spinal cord of amyotrophic lateral sclerosis, *Synapse 45*, 245−249.
19. Kawahara, Y., Ito, K., Sun, H., Aizawa, H., Kanazawa, I., and Kwak, S. (2004) Glutamate receptors: RNA editing and death of motor neurons, *Nature 427*, 801.
20. Shi, S., Hayashi, Y., Esteban, J. A., and Malinow, R. (2001) Subunit-specific rules governing AMPA receptor trafficking to synapses in hippocampal pyramidal neurons, *Cell 105*, 331−343.
21. Zhu, J. J., Esteban, J. A., Hayashi, Y., and Malinow, R. (2000) Postnatal synaptic potentiation: Delivery of GluR4-containing AMPA receptors by spontaneous activity, *Nat. Neurosci. 3*, 1098−1106.
22. Rogers, S. W., Andrews, P. I., Gahring, L. C., Whisenand, T., Cauley, K., Crain, B., Hughes, T. E., Heinemann, S. F., and McNamara, J. O. (1994) Autoantibodies to glutamate receptor GluR3 in Rasmussen's encephalitis, *Science 265*, 648−651.
23. Mantegazza, R., Bernasconi, P., Baggi, F., Spreafico, R., Ragona, F., Antozzi, C., Bernardi, G., and Granata, T. (2002) Antibodies against GluR3 peptides are not specific for Rasmussen's encephalitis but are also present in epilepsy patients with severe, early onset disease and intractable seizures, *J. Neuroimmunol. 131*, 179−185.
24. Ganor, Y., Besser, M., Ben-Zakay, N., Unger, T., and Levite, M. (2003) Human T cells express a functional ionotropic glutamate receptor GluR3, and glutamate by itself triggers integrin-mediated adhesion to laminin and fibronectin and chemotactic migration, *J. Immunol. 170*, 4362−4372.
25. Rembach, A., Turner, B. J., Bruce, S., Cheah, I. K., Scott, R. L., Lopes, E. C., Zagami, C. J., Beart, P. M., Cheung, N. S., Langford, S. J., and Cheema, S. S. (2004) Antisense peptide nucleic acid targeting GluR3 delays disease onset and progression in the SOD1 G93A mouse model of familial ALS, *J. Neurosci. Res. 77*, 573−582.
26. Swanson, G. T., Kamboj, S. K., and Cull-Candy, S. G. (1997) Single-channel properties of recombinant AMPA receptors depend on RNA editing, splice variation, and subunit composition, *J. Neurosci. 17*, 58−69.
27. Derkach, V., Barria, A., and Soderling, T. R. (1999) Ca^{2+}/calmodulin-kinase II enhances channel conductance of α-amino-3-hydroxy-5-methyl-4-isoxazolepropionate type glutamate receptors, *Proc. Natl. Acad. Sci. U.S.A. 96*, 3269−3274.
28. Jin, R., Banke, T. G., Mayer, M. L., Traynelis, S. F., and Gouaux, E. (2003) Structural basis for partial agonist action at ionotropic glutamate receptors, *Nat. Neurosci. 6*, 803−810.
29. Wieboldt, R., Gee, K. R., Niu, L., Ramesh, D., Carpenter, B. K., and Hess, G. P. (1994) Photolabile precursors of glutamate: Synthesis, photochemical properties, and activation of glutamate receptors on a microsecond time scale, *Proc. Natl. Acad. Sci. U.S.A. 91*, 8752−8756.
30. Li, G., Pei, W., and Niu, L. (2003) Channel-opening kinetics of $GluR2Q_{flip}$ AMPA receptor: A laser-pulse photolysis study, *Biochemistry 42*, 12358−12366.
31. Li, G., and Niu, L. (2004) How fast does the GluR1Qflip channel open? *J. Biol. Chem. 279*, 3990−3997.
32. Li, G., Sheng, Z., Huang, Z., and Niu, L. (2005) Kinetic mechanism of channel opening of the GluRDflip AMPA receptor, *Biochemistry 44*, 5835−5841.
33. Huang, Z., Li, G., Pei, W., Sosa, L. A., and Niu, L. (2005) Enhancing protein expression in single HEK 293 cells, *J. Neurosci. Methods 142*, 159−166.
34. Udgaonkar, J. B., and Hess, G. P. (1987) Chemical kinetic measurements of a mammalian acetylcholine receptor by a fast-reaction technique, *Proc. Natl. Acad. Sci. U.S.A. 84*, 8758−8762.
35. Longsworth, L. G. (1953) Diffusion measurements at 25° of aqueous solutions of amino acids, peptides and sugars, *J. Am. Chem. Soc. 75*, 5705−5709.
36. Watase, K., Sekiguchi, M., Matsui, T. A., Tagawa, Y., and Wada, K. (1997) Dominant negative mutant of ionotropic glutamate receptor subunit GluR3: Implications for the role of a cysteine residue for its channel activity and pharmacological properties, *Biochem. J. 322*, 385−391.
37. Quirk, J. C., and Nisenbaum, E. S. (2003) Multiple molecular determinants for allosteric modulation of alternatively spliced AMPA receptors, *J. Neurosci. 23*, 10953−10962.
38. Stern-Bach, Y., Russo, S., Neuman, M., and Rosenmund, C. (1998) A point mutation in the glutamate binding site blocks desensitization of AMPA receptors, *Neuron 21*, 907−918.
39. Chen, W., and Hahn, W. C. (2003) SV40 early region oncoproteins and human cell transformation, *Histol. Histopathol. 18*, 541−550.
40. Rosenmund, C., Stern-Bach, Y., and Stevens, C. F. (1998) The tetrameric structure of a glutamate receptor channel, *Science 280*, 1596−1599.
41. Armstrong, N., and Gouaux, E. (2000) Mechanisms for activation and antagonism of an AMPA-sensitive glutamate receptor: Crystal structures of the GluR2 ligand binding core, *Neuron 28*, 165−181.
42. Loftfield, R. B., and Eigner, E. A. (1969) Molecular order of participation of inhibitors (or activators) in biological systems, *Science 164*, 305−308.
43. Koike, M., Tsukada, S., Tsuzuki, K., Kijima, H., and Ozawa, S. (2000) Regulation of kinetic properties of GluR2 AMPA receptor channels by alternative splicing, *J. Neurosci. 20*, 2166−2174.
44. Raman, I. M., and Trussell, L. O. (1995) The mechanism of α-amino-3-hydroxy-5-methyl-4-isoxazolepropionate receptor desensitization after removal of glutamate, *Biophys. J. 68*, 137−146.
45. Vyklicky, L., Jr., Patneau, D. K., and Mayer, M. L. (1991) Modulation of excitatory synaptic transmission by drugs that reduce desensitization at AMPA/kainate receptors, *Neuron 7*, 971−984.
46. Heckmann, M., Bufler, J., Franke, C., and Dudel, J. (1996) Kinetics of homomeric GluR6 glutamate receptor channels, *Biophys. J. 71*, 1743−1750.
47. Jin, R., Horning, M., Mayer, M. L., and Gouaux, E. (2002) Mechanism of activation and selectivity in a ligand-gated ion channel: Structural and functional studies of GluR2 and quisqualate, *Biochemistry 41*, 15635−15643.
48. Smith, T. C., and Howe, J. R. (2000) Concentration-dependent substate behavior of native AMPA receptors, *Nat. Neurosci. 3*, 992−997.
49. Mayer, M. L., and Armstrong, N. (2004) Structure and function of glutamate receptor ion channels, *Annu. Rev. Physiol. 66*, 161−181.
50. Clements, J. D., Lester, R. A., Tong, G., Jahr, C. E., and Westbrook, G. L. (1992) The time course of glutamate in the synaptic cleft, *Science 258*, 1498−1501.

51. Diamond, J. S., and Jahr, C. E. (1997) Transporters buffer synaptically released glutamate on a submillisecond time scale, *J. Neurosci. 17*, 4672−4687.
52. Traynelis, S. F., and Wahl, P. (1997) Control of rat GluR6 glutamate receptor open probability by protein kinase A and calcineurin, *J. Physiol. 503*, 513−531.
53. Matsubara, N., Billington, A. P., and Hess, G. P. (1992) How fast does an acetylcholine receptor channel open? Laser-pulse photolysis of an inactive precursor of carbamoylcholine in the microsecond time region with BC3H1 cells, *Biochemistry 31*, 5507−5514.
54. Colquhoun, D., Jonas, P., and Sakmann, B. (1992) Action of brief pulses of glutamate on AMPA/kainate receptors in patches from different neurones of rat hippocampal slices, *J. Physiol. 458*, 261−287.
55. Nielsen, T. A., DiGregorio, D. A., and Silver, R. A. (2004) Modulation of glutamate mobility reveals the mechanism underlying slow-rising AMPAR EPSCs and the diffusion coefficient in the synaptic cleft, *Neuron 42*, 757−771.
56. Renger, J. J., Egles, C., and Liu, G. (2001) A developmental switch in neurotransmitter flux enhances synaptic efficacy by affecting AMPA receptor activation, *Neuron 29*, 469−484.
57. Armstrong, N., Mayer, M., and Gouaux, E. (2003) Tuning activation of the AMPA-sensitive GluR2 ion channel by genetic adjustment of agonist-induced conformational changes, *Proc. Natl. Acad. Sci. U.S.A. 100*, 5736−5741.
58. Sun, Y., Olson, R., Horning, M., Armstrong, N., Mayer, M., and Gouaux, E. (2002) Mechanism of glutamate receptor desensitization, *Nature 417*, 245−253.
59. Fersht, A. (1999) *Structure and Mechanism in Protein Science*, W. H. Freeman, New York.
60. Trussell, L. O., and Fischbach, G. D. (1989) Glutamate receptor desensitization and its role in synaptic transmission, *Neuron 3*, 209−218.
61. Choi, S., Klingauf, J., and Tsien, R. W. (2000) Postfusional regulation of cleft glutamate concentration during LTP at 'silent synapses', *Nat. Neurosci. 3*, 330−336.
62. Carter, A. G., and Regehr, W. G. (2000) Prolonged synaptic currents and glutamate spillover at the parallel fiber to stellate cell synapse, *J. Neurosci. 20*, 4423−4434.
63. Schoppa, N. E., and Westbrook, G. L. (2001) Glomerulus-specific synchronization of mitral cells in the olfactory bulb, *Neuron 31*, 639−651.
64. Galarreta, M., and Hestrin, S. (2001) Spike transmission and synchrony detection in networks of GABAergic interneurons, *Science 292*, 2295−2299.
65. Cathala, L., Brickley, S., Cull-Candy, S., and Farrant, M. (2003) Maturation of EPSCs and intrinsic membrane properties enhances precision at a cerebellar synapse, *J. Neurosci. 23*, 6074−6085.
66. Mitchell, S. J., and Silver, R. A. (2003) Shunting inhibition modulates neuronal gain during synaptic excitation, *Neuron 38*, 433−445.
67. Li, G., Oswald, R. E., and Niu, L. (2003) Channel-opening kinetics of GluR6 kainate receptor, *Biochemistry 42*, 12367−12375.
68. Wyllie, D. J., Behe, P., and Colquhoun, D. (1998) Single-channel activations and concentration jumps: Comparison of recombinant NR1a/NR2A and NR1a/NR2D NMDA receptors, *J. Physiol. 510*, 1−18.
69. Robert, A., and Howe, J. R. (2003) How AMPA receptor desensitization depends on receptor occupancy, *J. Neurosci. 23*, 847−858.

BI062213S